



This is the accepted manuscript made available via CHORUS. The article has been published as:

Optical Trapping of a Polyatomic Molecule in an  $\ell$ -Type Parity Doublet State

Christian Hallas, Nathaniel B. Vilas, Loïc Anderegg, Paige Robichaud, Andrew Winnicki, Chaoqun Zhang, Lan Cheng, and John M. Doyle

Phys. Rev. Lett. **130**, 153202 — Published 14 April 2023

DOI: [10.1103/PhysRevLett.130.153202](https://doi.org/10.1103/PhysRevLett.130.153202)

# Optical Trapping of a Polyatomic Molecule in an $\ell$ -Type Parity Doublet State

Christian Hallas,<sup>1,2,\*</sup> Nathaniel B. Vilas,<sup>1,2</sup> Loïc Anderegg,<sup>1,2</sup> Paige Robichaud,<sup>1,2</sup>  
Andrew Winnicki,<sup>1,2</sup> Chaoqun Zhang,<sup>3</sup> Lan Cheng,<sup>3</sup> and John M. Doyle<sup>1,2</sup>

<sup>1</sup>*Department of Physics, Harvard University, Cambridge, MA 02138, USA*

<sup>2</sup>*Harvard-MIT Center for Ultracold Atoms, Cambridge, MA 02138, USA*

<sup>3</sup>*Department of Chemistry, The Johns Hopkins University, Baltimore, MD 21218, USA*

(Dated: March 9, 2023)

We report optical trapping of a polyatomic molecule, calcium monohydroxide (CaOH). CaOH molecules from a magneto-optical trap are sub-Doppler laser cooled to  $20(3) \mu\text{K}$  in free space and loaded into an optical dipole trap. We attain an in-trap molecule number density of  $3(1) \times 10^9 \text{ cm}^{-3}$  at a temperature of  $57(8) \mu\text{K}$ . Trapped CaOH molecules are optically pumped into an excited vibrational bending mode, whose  $\ell$ -type parity doublet structure is a potential resource for a wide range of proposed quantum science applications with polyatomic molecules. We measure the spontaneous, radiative lifetime of this bending mode state to be  $\sim 0.7$  s.

Ultracold molecules are a promising platform for pursuing a large and diverse set of applications in quantum science [1]. Recent experimental progress has led to ultracold samples of a broad range of heteronuclear diatomic species, produced via either direct laser cooling [2–5] or assembly of ultracold atoms [6–12]. These experiments have enabled new advances in physics such as the realization of degenerate gases of polar molecules [13, 14] and novel studies of ultracold collisions [15–20]. Polyatomic molecules, as compared with diatomic molecules, have qualitatively richer internal level structures, which are expected to open up access to new, unique possibilities. Most prominently, polyatomic molecules generically possess low-lying, closely spaced levels with opposite parity. These parity doublets allow polyatomic molecules to be fully polarized at small electric fields, typically  $\sim 1$ – $100$  V/cm, resulting in long-lived quantum states with permanent electric dipole moments aligned in the lab frame [21–23]. These states are accompanied by states with zero lab-frame dipole moments. Such manifolds of states have been proposed for novel quantum simulation and computation platforms that have minimal field requirements and easily switchable interactions [22, 24–27], and for improved precision measurements of fundamental physics [21, 28, 29]. Ultracold polyatomic molecules would also facilitate new applications in beyond-standard-model searches [30], quantum chemistry [31–34], and ultracold collisions [35].

While offering new scientific capabilities, the internal complexity of polyatomic molecules also presents challenges to trapping and cooling. To date, only two species of polyatomic molecules, formaldehyde ( $\text{H}_2\text{CO}$ ) and calcium monohydroxide (CaOH), have been trapped and cooled below 1 mK, using optoelectrical cooling in an electric trap and direct laser cooling in a magneto-optical trap (MOT), respectively [36, 37]. Unlocking the many capabilities of polyatomic molecules will require techniques to reach even lower temperatures, as well as ways to attain long coherence times and high-fidelity quantum state control and readout. Optical trapping in particular has emerged as an important tool in ultracold physics for satisfying these criteria, as demonstrated by recent advances in quantum simulation and computation with neutral atoms [38–

42] and trapping of individual diatomic molecules in optical tweezers [43–46]. Developing methods to optically trap polyatomic molecules is highly desired in order to realize their full scientific and technological potential.

In this Letter, we report optical trapping of a polyatomic molecule, CaOH. Using a combination of two sub-Doppler laser cooling schemes, CaOH molecules are cooled to a temperature of  $20(3) \mu\text{K}$  in free space and loaded into an optical dipole trap (ODT). Efficient state transfer of the trapped CaOH molecules to the  $\tilde{X}^2\Sigma^+(010)(N'' = 1^-)$  [47] vibrational bending mode is accomplished via optical pumping. This state possesses an “ $\ell$ -type” parity doublet structure due to its near-degenerate vibrational angular momentum ( $\ell$ ) levels [48]. *Ab initio* calculations for the spontaneous, radiative lifetime of the  $\tilde{X}^2\Sigma^+(010)(N'' = 1^-)$  state,  $\tau_{\text{rad}}$ , are performed and agree well with our experimentally measured value of  $\tau_{\text{rad}} = 0.72^{+0.25}_{-0.13}$  s.

Our experiment starts with optical radiative slowing and magneto-optical trapping of CaOH molecules from a cryogenic buffer gas beam [55]. Photon cycling is realized by driving the  $\tilde{X}^2\Sigma^+(000)(N'' = 1) \rightarrow A^2\Pi_{1/2}(000)(J' = 1/2)$  electronic transition while optically repumping vibrational branching decay to eleven rovibrational states back to the cycling transition [37, 56, 57]. A detailed description of the apparatus and the repumping scheme is provided in Ref. [37]. In that previous work, we demonstrated sub-Doppler cooling of CaOH molecules to a temperature of  $\sim 110 \mu\text{K}$ . Here, we cool to lower temperatures by implementing two sub-Doppler cooling schemes in combination,  $\Lambda$ -cooling [5, 58] and single frequency (SF) cooling [3]. These cooling schemes have recently been used to cool diatomic molecules to  $5 \mu\text{K}$  [3] and rely on creating zero-velocity dark states to achieve velocity-selective coherent population trapping (VSCPT). In  $\Lambda$ -cooling, counter-propagating lasers couple two ground states to a single excited state; a zero-velocity dark state occurs when the lasers are tuned to two-photon resonance [59]. In SF cooling, the zero-velocity dark states are created in the presence of a single frequency component of light that is blue-detuned from relevant ground state levels [3].

Our  $\Lambda$ -cooling and SF cooling implementations for CaOH

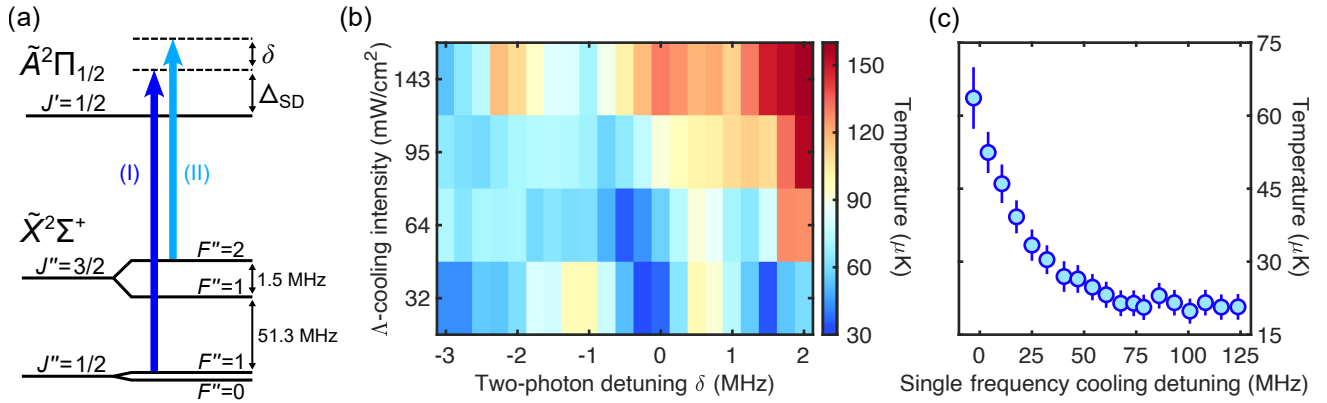


Figure 1.  $\Lambda$ -cooling and single frequency (SF) cooling of CaOH. (a) CaOH level structure and the two frequency components used for  $\Lambda$ -cooling (dark (I) and light blue (II) arrows), with a two-photon detuning of  $\delta$  and single photon detuning of  $\Delta_{SD}$ . For SF cooling, only the bluer component (I) is present. (b)  $\Lambda$ -cooling temperature as a function of  $\delta$  and intensity per cooling beam,  $I_{SD}$ . (c) Temperature of SF cooling as a function of  $\Delta_{SD}$  at  $I_{SD} = 64 \text{ mW/cm}^2$ . Error bars include  $1\sigma$  errors from the temperature fitting and systematic effects from imaging [49].

molecules are both based on creating a blue-detuned optical molasses that addresses the same  $\tilde{X}^2\Sigma^+ \rightarrow \tilde{A}^2\Pi_{1/2}$  transition as the MOT. This is a “type-II” transition (i.e.,  $J'' \geq J'$ ), which exhibits strong sub-Doppler cooling (heating) at blue (red) detuning due to polarization gradient forces that arise from the existence of dark states in the ground state manifold [60–63]. The experimental sequence for applying the molasses is as follows. Starting with CaOH molecules loaded into the MOT as described in Ref. [37], the molecular cloud is compressed to about half its size by ramping the MOT gradient over 5 ms, from 8.3 G/cm (its value during MOT loading) to 23.6 G/cm. The MOT laser beams, MOT coils, and MOT light polarization switching (which is used to remix magnetic dark states) are then turned off in a time period of 130  $\mu\text{s}$ . The two frequency components of the MOT beams—which separately address the spin-rotation components  $\tilde{X}^2\Sigma^+(N'' = 1, J'' = 1/2)$  and  $\tilde{X}^2\Sigma^+(N'' = 1, J'' = 3/2)$ —are simultaneously tuned to the blue of the optical transition. The laser beams are then quickly turned back on to form the “blue-detuned molasses.”

The blue-detuned molasses is configured for  $\Lambda$ -cooling by coupling two hyperfine levels in the  $\tilde{X}^2\Sigma^+(N'' = 1)$  manifold to the  $\tilde{A}^2\Pi_{1/2}(J' = 1/2)$  excited state. To achieve this, the two frequency components of the molasses are tuned to nominally address the  $\tilde{X}^2\Sigma^+(J'' = 3/2, F'' = 2)$  and  $\tilde{X}^2\Sigma^+(J'' = 1/2)$  levels (Fig. 1(a)), with polarizations  $\sigma^-$  and  $\sigma^+$ , respectively. (Hyperfine levels in the  $\tilde{X}^2\Sigma^+(J'' = 1/2)$  state are unresolved in our experiment [64].) Both frequency components are blue-detuned by a common detuning  $\Delta_{SD}$ , while the component addressing  $\tilde{X}^2\Sigma^+(J'' = 3/2, F'' = 2)$  is further detuned by  $\delta$ , the two-photon detuning. We set  $\Delta_{SD} = 12 \text{ MHz}$ , informed by our previous sub-Doppler cooling results in Ref. [37]. The peak cooling intensity,  $I_{SD}$ , is divided between the two frequency components, whose intensities are  $I_{SD}/3$  for  $\tilde{X}^2\Sigma^+(J'' = 3/2, F'' = 2)$  and  $2I_{SD}/3$  for  $\tilde{X}^2\Sigma^+(J'' = 1/2)$ .

We investigate the dependence of  $\Lambda$ -cooling on both  $\delta$  and

$I_{SD}$ , using ballistic expansion of the cooled molecules to measure their temperature after 1 ms of  $\Lambda$ -cooling (Fig. 1(b)) [49]. This cooling duration was chosen to be many times longer than the characteristic time of the cooling. The lowest measured temperature,  $T_{\min} = 34(3) \mu\text{K}$ , occurs at  $\delta \approx 0 \text{ MHz}$  and at the lowest cooling intensity used,  $I_{SD} = 32 \text{ mW/cm}^2$ . A second, slightly higher local temperature minimum is observed at  $\delta \approx 1.5 \text{ MHz}$ , which corresponds to the two-photon resonance for the  $\Lambda$ -system consisting of  $\tilde{X}^2\Sigma^+(J'' = 3/2, F'' = 1)$  and  $\tilde{X}^2\Sigma^+(J'' = 1/2)$ . At higher intensities, the temperature is minimized at increasingly negative  $\delta$ . We attribute this behavior to ac Stark shifts of the  $\Lambda$ -coupled hyperfine levels due to the cooling light: for higher intensities, the levels move further apart, and smaller  $\delta$  is required to satisfy the two-photon resonance condition.

SF cooling is implemented similarly to  $\Lambda$ -cooling, except that the frequency component used to address the  $\tilde{X}^2\Sigma^+(J'' = 3/2, F'' = 2)$  state is removed. We find that the capture velocity of SF cooling is too low to cool molecules directly from the

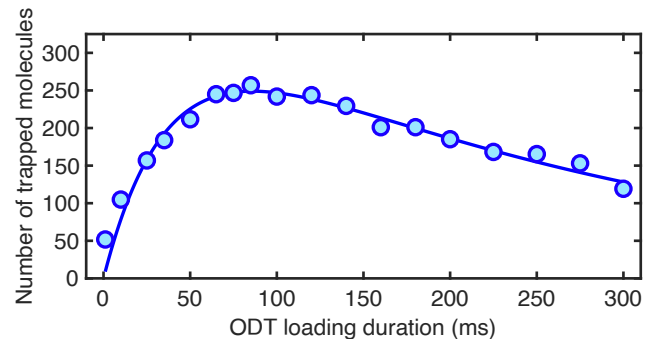


Figure 2. Number of CaOH molecules loaded into the optical dipole trap versus duration of ODT loading with SF cooling on. The solid curve is a fit to a rate equation with constant loading and loss rates. The loss rate is consistent with loss to vibrational dark states during SF cooling. Error bars are smaller than the data points.

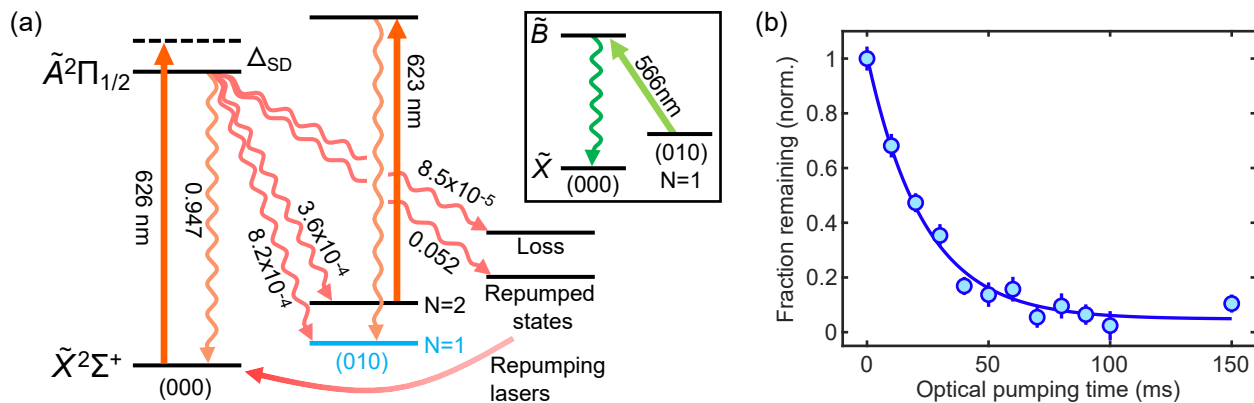


Figure 3. Populating the  $\tilde{X}^2\Sigma^+(010)(N'' = 1)$  vibrational bending mode. (a) The optical pumping scheme. The bending mode repumping laser is turned off while all other cycling and repumping lasers remain on. Vibrational repumping lasers for other states are shown schematically by the “repumping” arrow connecting back to (000). Vibrational branching ratios are labeled for each decay channel. The main cooling laser is blue-detuned by a frequency  $\Delta_{SD}$  to perform SF cooling of the molecules during population transfer. For more details on the optical cycling lasers used, see Ref. [37]. Inset: repumping transition driven to optically detect molecules in the bending mode. (b) Transfer into the bending mode versus optical pumping time. The solid curve is an exponential fit with a time constant of  $\tau = 23.4(2.2)$  ms.

MOT temperature of  $\sim 0.8$  mK. We therefore start by cooling the molecular cloud with  $\Lambda$ -cooling, then apply SF cooling. For this sequence of cooling,  $\Lambda$ -cooling with parameters of  $\Delta_{SD} = 10$  MHz,  $\delta = 0.25$  MHz, and  $I_{SD} = 32$  mW/cm<sup>2</sup> is applied for 2 ms, which cools the molecular cloud to  $T \approx 50$   $\mu$ K. The molasses is next reconfigured for SF cooling in a period of 1 ms, during which time the molasses light is turned off. SF cooling is then applied for 5 ms, resulting in a minimum temperature of  $T_{min} = 20(3)$   $\mu$ K, realized when  $I_{SD} = 64$  mW/cm<sup>2</sup> and  $\Delta_{SD} \gtrsim 70$  MHz (Fig. 1(c)). The cooling efficiency is insensitive to detuning above some threshold ( $\Delta_{SD} \approx 70$  MHz), as has also been observed in SF cooling of CaF molecules [3].

CaOH molecules are loaded into the ODT using the blue-detuned molasses. The trapping potential is formed by a 1064 nm Gaussian laser beam with a power of 13.3 W and waist of  $\sim 25$   $\mu$ m. *Ab initio* calculations of the polarizability of the  $\tilde{X}^2\Sigma^+$  state predict a trap depth of  $\sim 600$   $\mu$ K, which agrees well with the trap depth we measure using radial trap frequencies [49]. The experimental sequence is as follows. After switching off the MOT, the ODT is turned on and a 1 ms pulse of  $\Lambda$ -cooling ( $\Delta_{SD} = 12$  MHz,  $\delta = 0$  MHz,  $I_{SD} = 64$  mW/cm<sup>2</sup>) is used to cool the molecules to below the capture velocity of SF cooling. The molasses is then reconfigured for SF cooling ( $\Delta_{SD} = 74$  MHz,  $I_{SD} = 64$  mW/cm<sup>2</sup>) to cool and load the molecules into the ODT. After loading the ODT, the molasses is turned off for 50 ms to allow untrapped molecules to escape the field of view of the EMCCD camera used to image the molecules. Trapped molecules are then imaged by turning SF cooling on again for 100 ms and collecting fluorescence decays from the  $\tilde{B}^2\Sigma^+$  state [37]. We find that a maximum number of 260(80) molecules are trapped in the ODT by loading with SF cooling for  $\sim 80$  ms (Fig. 2). Longer loading times decrease the number of loaded molecules due to loss to rovibrational dark states during SF cooling. An in-trap temperature of  $T = 57(8)$   $\mu$ K is determined by varying the ODT depth and

observing the number of surviving molecules [49]. We calculate a peak molecule number density of  $3(1) \times 10^9$  cm<sup>-3</sup> and a phase-space density of  $9(5) \times 10^{-8}$  in the ODT [65].

To study the  $\tilde{X}^2\Sigma^+(010)(N'' = 1^-)$  vibrational bending mode, we optically pump molecules into this state by simply turning off the corresponding repumping laser (Fig. 3(a)). To quantify the transfer, we first load the ODT and image the trapped molecules with 50 ms of SF cooling, as described above. This first image serves as a normalization signal to account for shot-to-shot variations in the number of molecules loaded into the ODT. The molecules are then SF cooled for a variable time with the  $\tilde{X}^2\Sigma^+(010)(N'' = 1^-)$  repumping laser turned off. The vibrational branching ratio (VBR) from the optical cycle into this state is  $v_{bend} = 8.2 \times 10^{-4}$ , while the VBR into dark rovibrational states is  $v_{dark} \approx 8.5 \times 10^{-5}$  [37]. We therefore expect the fraction of molecules pumped into the vibrational bending mode to be at most  $v_{bend}/(v_{bend} + v_{dark}) \approx 91\%$ . The timescale for optical pumping,  $\tau_{bend}$ , corresponds to  $1/v_{bend} \approx 1200$  photons scattered at the SF cooling scattering rate,  $R_{SF}$ . At the measured scattering rate of  $R_{SF} = 45 \times 10^3$  s<sup>-1</sup> [49], this results in a calculated optical pumping timescale of  $\sim 26$  ms. After optical pumping, the surviving ground-state molecules are imaged with the bending mode repumping laser turned off (Fig. 3(b)). We observe  $\tau_{bend} = 23.4(2.2)$  ms, which is consistent with the calculated value. A short repumping pulse on the  $\tilde{X}^2\Sigma^+(010)(N'' = 1^-) \rightarrow \tilde{B}^2\Sigma^+(000)(N' = 0)$  transition is used to recover molecules from the bending mode (Fig. 3(a), inset). We observe 80(3)% survival after two-way transfer into and out of the bending mode, normalized to the number of surviving molecules after an equal hold time in the  $\tilde{X}^2\Sigma^+(000)$  ground state. There is no measurable change to the in-trap temperature due to the optical pumping, hence the density in the trap has decreased by at most  $\sim 20\%$  after the transfer.

We measure the radiative lifetime of the  $\tilde{X}^2\Sigma^+(010)$  vibra-

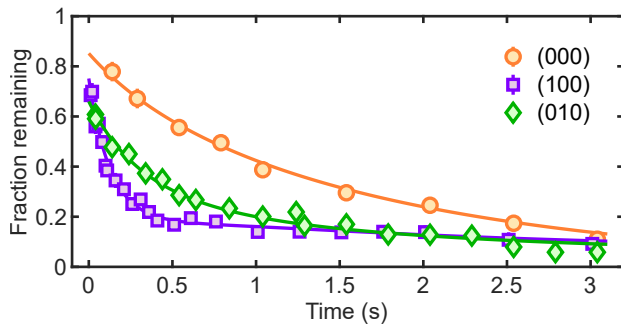


Figure 4. Lifetime of optically trapped CaOH molecules in the  $\tilde{X}^2\Sigma^+(000)$ ,  $\tilde{X}^2\Sigma^+(010)$ , and  $\tilde{X}^2\Sigma^+(100)$  vibrational states. Data points are the fraction of molecules remaining in detectable rovibrational states after holding them in the ODT for a variable time following transfer to the ( $N'' = 1^-$ ) level of the target vibrational state. Solid curves are fits to the rate equation model described in the text.

tional bending mode,  $\tau_{\text{rad}}$ . The measurement sequence starts by optically pumping into the bending mode for 100 ms and then holding the molecules in the ODT for a variable duration with all cooling and repumping lasers off. The surviving detectable molecules, which include all molecules in the ( $N'' = 1^-$ ) level of the bending mode along with all other repumped vibrational states [37], are then imaged for 50 ms. The surviving fraction, normalized to the number of molecules imaged before state transfer, is shown as a function of time in Fig. 4. Similar measurements are made for the  $\tilde{X}^2\Sigma^+(000)$  and  $\tilde{X}^2\Sigma^+(100)$  vibrational states. The dominant mechanism for the observed loss for the  $\tilde{X}^2\Sigma^+(010)$  and  $\tilde{X}^2\Sigma^+(100)$  states is radiative decay to the  $\tilde{X}^2\Sigma^+(000)$  ( $N'' = 0$ ) and  $\tilde{X}^2\Sigma^+(000)$  ( $N'' = 2$ ) rotational states, which are undetected (but still trapped). Losses due to blackbody excitation between rovibrational states and vacuum loss occur at similar timescales and are the primary cause for the observed loss for the  $\tilde{X}^2\Sigma^+(000)$  state. In order to isolate the separate decay mechanisms, the data for all three states are fit to a rate equation model (solid curves) incorporating all these effects. The rate equations capture the evolution of the vibrational populations over two distinct timescales: (i) initial vibrational thermalization due to radiative decay and blackbody excitation, and (ii) slow losses induced by blackbody excitation and vacuum loss. A detailed description of the model is provided in Ref. [66]. The fitted lifetime of the  $\tilde{X}^2\Sigma^+(010)$  state, including all losses, is  $0.36^{+0.11}_{-0.07}$  s (68% confidence interval), while the radiative lifetime determined from the fit is  $\tau_{\text{rad}} = 0.72^{+0.25}_{-0.13}$  s. The measured lifetime of the  $\tilde{X}^2\Sigma^+(000)$  state is  $0.90^{+0.20}_{-0.16}$  s, dominated by the  $1.3^{+0.3}_{-0.2}$  s timescale for blackbody excitation to  $\tilde{X}^2\Sigma^+(010)$  and  $\tilde{X}^2\Sigma^+(100)$ . The lifetime of  $\tilde{X}^2\Sigma^+(100)$  is  $0.14^{+0.02}_{-0.02}$  s, dominated by the  $0.19^{+0.03}_{-0.03}$  s lifetime for spontaneous, radiative decay to  $\tilde{X}^2\Sigma^+(000)$ . The fitted vacuum lifetime is  $3.0^{+0.4}_{-0.7}$  s.

We perform *ab initio* calculations for the radiative lifetime of the  $\tilde{X}^2\Sigma^+(010)$  state of CaOH and compare with our experimental measurement. Details on these calculations are

provided in Ref. [66]. In brief, the calculations include anharmonic contributions and employ high-level treatments of electron correlation. The transition dipole moments between vibrational states of  $\tilde{X}^2\Sigma^+$  were calculated using an equation-of-motion coupled-cluster (EOM-CC) [67, 68] dipole moment surface and vibrational wave functions obtained from discrete variable representation [57, 69] calculations on an EOM-CC potential energy surface. The calculated radiative lifetime of  $\tau_{\text{rad}} = 0.88$  s agrees well with the measured value. The same computational protocol produced similar and slightly longer  $\tilde{X}^2\Sigma^+(010)$  spontaneous lifetimes for SrOH and YbOH [49], suggesting that  $\sim 1$  s coherence times are attainable in several other molecules with similar vibrational structure to CaOH.

In summary, we have sub-Doppler cooled CaOH molecules to a temperature of  $20(3)$   $\mu\text{K}$ , loaded them into an ODT, and transferred them into the long-lived  $\tilde{X}^2\Sigma^+(010)$  vibrational bending mode. The closely spaced  $\ell$ -type parity doublets in the bending mode allow the molecules to be fully polarized at  $\sim 300$  V/cm and should enable dipolar interactions [25, 27, 35], including applications that benefit from the existence of states with zero lab-frame electric dipole moment alongside strongly interacting states with Debye-level lab-frame dipole moments [22]. The spontaneous, radiative lifetime of the  $\tilde{X}^2\Sigma^+(010)$  bending mode is measured to be  $\tau_{\text{rad}} \approx 0.7$  s. This suggests that experiments with coherence times near  $\sim 1$  s are achievable for vibrational bending modes in molecules of this type, provided that technical sources of loss are addressed, e.g., by performing experiments in a mild cryogenic environment to suppress blackbody losses. Lifetimes of  $\sim 0.4$  s are currently attainable without apparatus upgrades. This also signals the potential of optically trapped molecules for spectroscopic measurements that would be difficult in a traditional beam-based apparatus, including their possible application to blackbody thermometry [70].

Optical trapping of polyatomic molecules opens paths to new precision measurements, including searches for dark matter [30] and the electron electric dipole moment [21]. In addition, the density of trapped CaOH molecules achieved here is sufficient for loading into optical tweezer arrays [43, 46], which would enable high-fidelity internal state manipulation of individual polyatomic molecules, controlled dipolar interactions between molecules in nearby traps, and studies of few-body interactions between molecules sharing a single trap [15, 17]. Molecule number densities two to three orders of magnitude higher could likely be achieved with improved ODT loading (e.g., using repulsive bottle-shaped traps [71]) and/or smaller trap geometries and would allow new studies of collisions [35] and ultracold chemistry [33, 34]. Studies of bulk dipolar gases may also be possible but will require phase-space densities close to quantum degeneracy [72, 73]. These phase-space densities might be achievable with evaporative cooling using microwave shielding, as demonstrated recently with diatomic molecules [14, 17]. Finally, this work suggests that optical trapping may be viable for several large classes of polyatomic molecules for which optical cycling is expected to be possible [74], ranging from MOR type molecules [75]

(of which several have already been laser cooled in one dimension [76–78]) to asymmetric molecules [23], and possibly more complex species [79–82]. Several of these species (e.g., CaSH and CaOCH<sub>3</sub>) have closely-spaced parity doublet states that are expected to have even longer radiative lifetimes (>10 s) than the  $\tilde{X}^2\Sigma^+(010)$  state in CaOH.

This work was supported by the AFOSR and the NSF. NBV acknowledges support from the NDSEG fellowship, LA from the HQI, and PR from the NSF GRFP. The computational work at Johns Hopkins University was supported by the NSF under Grant No. PHY-2011794.

---

\* christianhallas@g.harvard.edu

- [1] L. D. Carr, D. DeMille, R. V. Krems, and J. Ye, Cold and ultracold molecules: science, technology and applications, *New J. Phys.* **11**, 055049 (2009).
- [2] L. Anderegg, B. L. Augenbraun, Y. Bao, S. Burchesky, L. W. Cheuk, W. Ketterle, and J. M. Doyle, Laser cooling of optically trapped molecules, *Nat. Phys.* **14**, 890 (2018).
- [3] L. Caldwell, J. A. Devlin, H. J. Williams, N. J. Fitch, E. A. Hinds, B. E. Sauer, and M. R. Tarbutt, Deep Laser Cooling and Efficient Magnetic Compression of Molecules, *Phys. Rev. Lett.* **123**, 033202 (2019).
- [4] S. Ding, Y. Wu, I. A. Finneran, J. J. Burau, and J. Ye, Sub-Doppler Cooling and Compressed Trapping of YO Molecules at  $\mu$ K Temperatures, *Phys. Rev. X* **10**, 021049 (2020).
- [5] T. K. Langin, V. Jorapur, Y. Zhu, Q. Wang, and D. DeMille, Polarization Enhanced Deep Optical Dipole Trapping of  $\Lambda$ -Cooled Polar Molecules, *Phys. Rev. Lett.* **127**, 163201 (2021).
- [6] J. J. Zirbel, K.-K. Ni, S. Ospelkaus, T. L. Nicholson, M. L. Olsen, P. S. Julienne, C. E. Wieman, J. Ye, and D. S. Jin, Heteronuclear molecules in an optical dipole trap, *Phys. Rev. A* **78**, 013416 (2008).
- [7] K.-K. Ni, S. Ospelkaus, M. De Miranda, A. Pe’Er, B. Neyenhuis, J. Zirbel, S. Kotochigova, P. Julienne, D. Jin, and J. Ye, A High Phase-Space-Density Gas of Polar Molecules, *Science* **322**, 231 (2008).
- [8] M. P. Köppinger, D. J. McCarron, D. L. Jenkin, P. K. Molony, H.-W. Cho, S. L. Cornish, C. R. Le Sueur, C. L. Blackley, and J. M. Hutson, Production of optically trapped <sup>87</sup>RbCs Feshbach molecules, *Phys. Rev. A* **89**, 033604 (2014).
- [9] T. Takekoshi, L. Reichsöllner, A. Schindewolf, J. M. Hutson, C. R. Le Sueur, O. Dulieu, F. Ferlaino, R. Grimm, and H.-C. Nägerl, Ultracold Dense Samples of Dipolar RbCs Molecules in the Rovibrational and Hyperfine Ground State, *Phys. Rev. Lett.* **113**, 205301 (2014).
- [10] J. W. Park, S. A. Will, and M. W. Zwierlein, Ultracold Dipolar Gas of Fermionic <sup>23</sup>Na<sup>40</sup>K Molecules in Their Absolute Ground State, *Phys. Rev. Lett.* **114**, 205302 (2015).
- [11] K. K. Voges, P. Gersema, M. Meyer zum Alten Borgloh, T. A. Schulze, T. Hartmann, A. Zenesini, and S. Ospelkaus, Ultracold Gas of Bosonic <sup>23</sup>Na<sup>39</sup>K Ground-State Molecules, *Phys. Rev. Lett.* **125**, 083401 (2020).
- [12] Y. Yu, K. Wang, J. D. Hood, L. R. B. Picard, J. T. Zhang, W. B. Cairncross, J. M. Hutson, R. Gonzalez-Ferez, T. Rosenband, and K.-K. Ni, Coherent Optical Creation of a Single Molecule, *Phys. Rev. X* **11**, 031061 (2021).
- [13] L. De Marco, G. Valtolina, K. Matsuda, W. G. Tobias, J. P. Covey, and J. Ye, A degenerate Fermi gas of polar molecules, *Science* **363**, 853 (2019).
- [14] A. Schindewolf, R. Bause, X.-Y. Chen, M. Duda, T. Karman, I. Bloch, and X.-Y. Luo, Evaporation of microwave-shielded polar molecules to quantum degeneracy, *Nature* **607**, 677 (2022).
- [15] L. W. Cheuk, L. Anderegg, Y. Bao, S. Burchesky, S. S. Yu, W. Ketterle, K.-K. Ni, and J. M. Doyle, Observation of Collisions between Two Ultracold Ground-State CaF Molecules, *Phys. Rev. Lett.* **125**, 043401 (2020).
- [16] S. Jurgilas, A. Chakraborty, C. J. H. Rich, L. Caldwell, H. J. Williams, N. J. Fitch, B. E. Sauer, M. D. Frye, J. M. Hutson, and M. R. Tarbutt, Collisions between Ultracold Molecules and Atoms in a Magnetic Trap, *Phys. Rev. Lett.* **126**, 153401 (2021).
- [17] L. Anderegg, S. Burchesky, Y. Bao, S. S. Yu, T. Karman, E. Chae, K.-K. Ni, W. Ketterle, and J. M. Doyle, Observation of microwave shielding of ultracold molecules, *Science* **373**, 779 (2021).
- [18] P. D. Gregory, J. A. Blackmore, M. D. Frye, L. M. Fernley, S. L. Bromley, J. M. Hutson, and S. L. Cornish, Molecule–molecule and atom–molecule collisions with ultracold RbCs molecules, *New J. Phys.* **23**, 125004 (2021).
- [19] M. A. Nichols, Y.-X. Liu, L. Zhu, M.-G. Hu, Y. Liu, and K.-K. Ni, Detection of Long-Lived Complexes in Ultracold Atom-Molecule Collisions, *Phys. Rev. X* **12**, 011049 (2022).
- [20] W. G. Tobias, K. Matsuda, J.-R. Li, C. Miller, A. N. Carroll, T. Bilitewski, A. M. Rey, and J. Ye, Reactions between layer-resolved molecules mediated by dipolar spin exchange, *Science* **375**, 1299 (2022).
- [21] I. Kozyryev and N. R. Hutzler, Precision Measurement of Time-Reversal Symmetry Violation with Laser-Cooled Polyatomic Molecules, *Phys. Rev. Lett.* **119**, 133002 (2017).
- [22] P. Yu, L. W. Cheuk, I. Kozyryev, and J. M. Doyle, A scalable quantum computing platform using symmetric-top molecules, *New J. Phys.* **21**, 093049 (2019).
- [23] B. L. Augenbraun, J. M. Doyle, T. Zelevinsky, and I. Kozyryev, Molecular Asymmetry and Optical Cycling: Laser Cooling Asymmetric Top Molecules, *Phys. Rev. X* **10**, 031022 (2020).
- [24] Q. Wei, S. Kais, B. Friedrich, and D. Herschbach, Entanglement of polar symmetric top molecules as candidate qubits, *J. Chem. Phys.* **135**, 154102 (2011).
- [25] M. L. Wall, K. Maeda, and L. D. Carr, Simulating quantum magnets with symmetric top molecules, *Ann. Phys. (Berlin)* **525**, 845 (2013).
- [26] M. L. Wall, K. R. A. Hazzard, and A. M. Rey, Quantum Magnetism with Ultracold Molecules, in *From Atomic to Mesoscale: The Role of Quantum Coherence in Systems of Various Complexities*, edited by S. Malinovskaya and I. Novikova (World Scientific, 2015) Chap. 1, pp. 3–37.
- [27] M. L. Wall, K. Maeda, and L. D. Carr, Realizing unconventional quantum magnetism with symmetric top molecules, *New J. Phys.* **17**, 025001 (2015).
- [28] E. B. Norrgard, D. S. Barker, S. Eckel, J. A. Fedchak, N. N. Klimov, and J. Scherschligt, Nuclear-spin dependent parity violation in optically trapped polyatomic molecules, *Commun. Phys.* **2**, 77 (2019).
- [29] Y. Hao, P. Navrátil, E. B. Norrgard, M. Iliaš, E. Eliav, R. G. E. Timmermans, V. V. Flambaum, and A. Borschevsky, Nuclear spin-dependent parity-violating effects in light polyatomic molecules, *Phys. Rev. A* **102**, 052828 (2020).
- [30] I. Kozyryev, Z. Lasner, and J. M. Doyle, Enhanced sensitivity to ultralight bosonic dark matter in the spectra of the linear radical SrOH, *Phys. Rev. A* **103**, 043313 (2021).
- [31] R. V. Krems, Cold controlled chemistry, *Phys. Chem. Chem. Phys.* **10**, 4079 (2008).

- [32] N. Balakrishnan, Perspective: Ultracold molecules and the dawn of cold controlled chemistry, *J. Chem. Phys.* **145**, 150901 (2016).
- [33] J. L. Bohn, A. M. Rey, and J. Ye, Cold molecules: Progress in quantum engineering of chemistry and quantum matter, *Science* **357**, 1002 (2017).
- [34] B. R. Heazlewood and T. P. Softley, Towards chemistry at absolute zero, *Nat. Rev. Chem.* **5**, 125 (2021).
- [35] L. D. Augustovičová and J. L. Bohn, Ultracold collisions of polyatomic molecules: CaOH, *New J. Phys.* **21**, 103022 (2019).
- [36] A. Prehn, M. Ibrügger, R. Glöckner, G. Rempe, and M. Zeppenfeld, Optoelectrical Cooling of Polar Molecules to Submillikelvin Temperatures, *Phys. Rev. Lett.* **116**, 063005 (2016).
- [37] N. B. Vilas, C. Hallas, L. Anderegg, P. Robichaud, A. Winnicki, D. Mitra, and J. M. Doyle, Magneto-optical trapping and sub-Doppler cooling of a polyatomic molecule, *Nature* **606**, 70 (2022).
- [38] H. Bernien, S. Schwartz, A. Keesling, H. Levine, A. Omran, H. Pichler, S. Choi, A. S. Zibrov, M. Endres, M. Greiner, V. Vuletić, and M. D. Lukin, Probing many-body dynamics on a 51-atom quantum simulator, *Nature* **551**, 579 (2017).
- [39] H. Levine, A. Keesling, G. Semeghini, A. Omran, T. T. Wang, S. Ebadi, H. Bernien, M. Greiner, V. Vuletić, H. Pichler, and M. D. Lukin, Parallel Implementation of High-Fidelity Multi-qubit Gates with Neutral Atoms, *Phys. Rev. Lett.* **123**, 170503 (2019).
- [40] I. S. Madjarov, J. P. Covey, A. L. Shaw, J. Choi, A. Kale, A. Cooper, H. Pichler, V. Schkolnik, J. R. Williams, and M. Endres, High-fidelity entanglement and detection of alkaline-earth Rydberg atoms, *Nature Physics* **16**, 857 (2020).
- [41] K.-N. Schymik, V. Lienhard, D. Barredo, P. Scholl, H. Williams, A. Browaeys, and T. Lahaye, Enhanced atom-by-atom assembly of arbitrary tweezer arrays, *Phys. Rev. A* **102**, 063107 (2020).
- [42] P. Scholl, M. Schuler, H. J. Williams, A. A. Eberharter, D. Barredo, K.-N. Schymik, V. Lienhard, L.-P. Henry, T. C. Lang, T. Lahaye, A. M. Läuchli, and A. Browaeys, Quantum simulation of 2D antiferromagnets with hundreds of Rydberg atoms, *Nature* **595**, 233 (2021).
- [43] L. Anderegg, L. W. Cheuk, Y. Bao, S. Burchesky, W. Ketterle, K.-K. Ni, and J. M. Doyle, An optical tweezer array of ultracold molecules, *Science* **365**, 1156 (2019).
- [44] W. B. Cairncross, J. T. Zhang, L. R. B. Picard, Y. Yu, K. Wang, and K.-K. Ni, Assembly of a Rovibrational Ground State Molecule in an Optical Tweezer, *Phys. Rev. Lett.* **126**, 123402 (2021).
- [45] S. Burchesky, L. Anderegg, Y. Bao, S. S. Yu, E. Chae, W. Ketterle, K.-K. Ni, and J. M. Doyle, Rotational Coherence Times of Polar Molecules in Optical Tweezers, *Phys. Rev. Lett.* **127**, 123202 (2021).
- [46] J. T. Zhang, L. R. B. Picard, W. B. Cairncross, K. Wang, Y. Yu, F. Fang, and K.-K. Ni, An optical tweezer array of ground-state polar molecules, *Quantum Sci. Technol.* **7**, 035006 (2022).
- [47] The notation  $(v_1 v_2 v_3)$  refers to the vibrational quanta in the three vibrational normal modes of CaOH, namely the Ca-O stretch, Ca-O-H bend, and O-H stretch modes, respectively.  $N$  is the rotational quantum number,  $J$  is the total angular momentum excluding nuclear spin, and  $F$  is the hyperfine quantum number. For electronic transitions, a prime ( $'$ ) refers to the excited state and a double prime ( $''$ ) refers to the ground state. A sign following the label (e.g.,  $N'' = 1^-$ ) refers to the parity of the state, and is specified explicitly in cases where parity may not otherwise be clear.
- [48]  $\ell$  is the projection of the vibrational orbital angular momentum in the bending mode onto the internuclear axis of the molecule. In  $\tilde{X}^2\Sigma^+(010)$ ,  $\ell$  can be  $-1$  or  $+1$ .
- [49] See Supplemental Material, which includes Refs. [50-54].
- [50] R. Grimm, M. Weidemüller, and Y. B. Ovchinnikov, Optical Dipole Traps for Neutral Atoms, in *Adv. At. Mol. Opt. Phys.*, Vol. 42, edited by B. Bederson and H. Walther (Academic Press, 2000) Chap. 4, pp. 95–170.
- [51] R. Simon, Anisotropic gaussian beams, *Opt. Commun.* **46**, 265 (1983).
- [52] P. R. Bevington and D. K. Robinson, *Data Reduction and Error Analysis for the Physical Sciences*, 3rd ed. (McGraw-Hill, New York, 2003).
- [53] J. Gauss and J. F. Stanton, Analytic CCSD(T) second derivatives, *Chem. Phys. Lett.* **276**, 70 (1997).
- [54] O. Christiansen, C. Hättig, and J. Gauss, Polarizabilities of CO, N<sub>2</sub>, HF, Ne, BH, and CH<sup>+</sup> from ab initio calculations: Systematic studies of electron correlation, basis set errors, and vibrational contributions, *J. Chem. Phys.* **109**, 4745 (1998).
- [55] N. R. Hutzler, H.-I. Lu, and J. M. Doyle, The Buffer Gas Beam: An Intense, Cold, and Slow Source for Atoms and Molecules, *Chem. Rev.* **112**, 4803 (2012).
- [56] L. Baum, N. B. Vilas, C. Hallas, B. L. Augenbraun, S. Raval, D. Mitra, and J. M. Doyle, Establishing a nearly closed cycling transition in a polyatomic molecule, *Phys. Rev. A* **103**, 043111 (2021).
- [57] C. Zhang, B. L. Augenbraun, Z. D. Lasner, N. B. Vilas, J. M. Doyle, and L. Cheng, Accurate prediction and measurement of vibronic branching ratios for laser cooling linear polyatomic molecules, *J. Chem. Phys.* **155**, 091101 (2021).
- [58] L. W. Cheuk, L. Anderegg, B. L. Augenbraun, Y. Bao, S. Burchesky, W. Ketterle, and J. M. Doyle,  $\Lambda$ -enhanced Imaging of Molecules in an Optical Trap, *Phys. Rev. Lett.* **121**, 083201 (2018).
- [59] A. Aspect, E. Arimondo, R. Kaiser, N. Vansteenkiste, and C. Cohen-Tannoudji, Laser Cooling below the One-Photon Recoil Energy by Velocity-Selective Coherent Population Trapping, *Phys. Rev. Lett.* **61**, 826 (1988).
- [60] C. Valentin, M.-C. Gagné, J. Yu, and P. Pillet, One-Dimension Sub-Doppler Molasses in the Presence of Static Magnetic Field, *Europhys. Lett.* **17**, 133 (1992).
- [61] D. Boiron, C. Triché, D. R. Meacher, P. Verkerk, and G. Grynberg, Three-dimensional cooling of cesium atoms in four-beam gray optical molasses, *Phys. Rev. A* **52**, R3425 (1995).
- [62] F. Sievers, N. Kretschmar, D. R. Fernandes, D. Suchet, M. Rabinovic, S. Wu, C. V. Parker, L. Khaykovich, C. Salomon, and F. Chevy, Simultaneous sub-Doppler laser cooling of fermionic <sup>6</sup>Li and <sup>40</sup>K on the  $D_1$  line: Theory and experiment, *Phys. Rev. A* **91**, 023426 (2015).
- [63] J. A. Devlin and M. R. Tarbutt, Three-dimensional Doppler, polarization-gradient, and magneto-optical forces for atoms and molecules with dark states, *New J. Phys.* **18**, 123017 (2016).
- [64] C. Scurlock, D. Fletcher, and T. Steimle, Hyperfine Structure in the  $(0, 0, 0)$   $\tilde{X}^2\Sigma^+$  State of CaOH Observed by Pump/Probe Microwave-Optical Double Resonance, *J. Mol. Spectrosc.* **159**, 350 (1993).
- [65] The unitless phase-space density is defined as  $\rho_0 = n_0 \lambda_{dB}^3$ , where  $n_0$  is the peak molecule number density and  $\lambda_{dB}$  is the deBroglie wavelength. We note that this definition does not account for the degrees of freedom associated with the internal state of the molecules. See ‘Supplemental Material’ for additional details.
- [66] N. B. Vilas, C. Hallas, L. Anderegg, P. Robichaud, C. Zhang, S. Dawley, L. Cheng, and J. M. Doyle, Blackbody thermalization and vibrational lifetimes of trapped polyatomic molecules

- (2023), to be published.
- [67] J. F. Stanton and R. J. Bartlett, The equation of motion coupled-cluster method. A systematic biorthogonal approach to molecular excitation energies, transition probabilities, and excited state properties, *J. Chem. Phys.* **98**, 7029 (1993).
- [68] M. Nooijen and R. J. Bartlett, Equation of motion coupled cluster method for electron attachment, *J. Chem. Phys.* **102**, 3629 (1995).
- [69] D. T. Colbert and W. H. Miller, A novel discrete variable representation for quantum mechanical reactive scattering via the S-matrix Kohn method, *J. Chem. Phys.* **96**, 1982 (1992).
- [70] E. B. Norrgard, S. P. Eckel, C. L. Holloway, and E. L. Shirley, Quantum blackbody thermometry, *New J. Phys.* **23**, 033037 (2021).
- [71] Y. Lu, C. M. Holland, and L. W. Cheuk, Molecular Laser Cooling in a Dynamically Tunable Repulsive Optical Trap, *Phys. Rev. Lett.* **128**, 213201 (2022).
- [72] T. Lahaye, C. Menotti, L. Santos, M. Lewenstein, and T. Pfau, The physics of dipolar bosonic quantum gases, *Rep. Prog. Phys.* **72**, 126401 (2009).
- [73] M. A. Baranov, M. Dalmonte, G. Pupillo, and P. Zoller, Condensed Matter Theory of Dipolar Quantum Gases, *Chem. Rev.* **112**, 5012 (2012).
- [74] T. A. Isaev and R. Berger, Polyatomic Candidates for Cooling of Molecules with Lasers from Simple Theoretical Concepts, *Phys. Rev. Lett.* **116**, 063006 (2016).
- [75] I. Kozyryev, L. Baum, K. Matsuda, and J. M. Doyle, Proposal for Laser Cooling of Complex Polyatomic Molecules, *ChemPhysChem* **17**, 3641 (2016).
- [76] I. Kozyryev, L. Baum, K. Matsuda, B. L. Augenbraun, L. Anderegg, A. P. Sedlack, and J. M. Doyle, Sisyphus Laser Cooling of a Polyatomic Molecule, *Phys. Rev. Lett.* **118**, 173201 (2017).
- [77] B. L. Augenbraun, Z. D. Lasner, A. Frenett, H. Sawaoka, C. Miller, T. C. Steimle, and J. M. Doyle, Laser-cooled polyatomic molecules for improved electron electric dipole moment searches, *New J. Phys.* **22**, 022003 (2020).
- [78] D. Mitra, N. B. Vilas, C. Hallas, L. Anderegg, B. L. Augenbraun, L. Baum, C. Miller, S. Raval, and J. M. Doyle, Direct laser cooling of a symmetric top molecule, *Science* **369**, 1366 (2020).
- [79] M. V. Ivanov, S. Gulania, and A. I. Krylov, Two Cycling Centers in One Molecule: Communication by Through-Bond Interactions and Entanglement of the Unpaired Electrons, *J. Phys. Chem. Lett.* **11**, 1297 (2020).
- [80] J. Kłos and S. Kotochigova, Prospects for laser cooling of polyatomic molecules with increasing complexity, *Phys. Rev. Res.* **2**, 013384 (2020).
- [81] C. E. Dickerson, H. Guo, A. J. Shin, B. L. Augenbraun, J. R. Caram, W. C. Campbell, and A. N. Alexandrova, Franck-Condon Tuning of Optical Cycling Centers by Organic Functionalization, *Phys. Rev. Lett.* **126**, 123002 (2021).
- [82] G.-Z. Zhu, D. Mitra, B. L. Augenbraun, C. E. Dickerson, M. J. Frim, G. Lao, Z. D. Lasner, A. N. Alexandrova, W. C. Campbell, J. R. Caram, J. M. Doyle, and E. R. Hudson, Functionalizing aromatic compounds with optical cycling centres, *Nat. Chem.* **595**, 233 (2021).